Bridge trisections and Seifert solids

JASON JOSEPH

JEFFREY MEIER

MAGGIE MILLER

ALEXANDER ZUPAN

We adapt Seifert's algorithm for classical knots and links to the setting of tri-plane diagrams for bridge trisected surfaces in the 4–sphere. Our approach allows for the construction of a Seifert solid that is described by a Heegaard diagram. The Seifert solids produced can be assumed to have exteriors that can be built without 3–handles; in contrast, we give examples of Seifert solids (not coming from our construction) whose exteriors require arbitrarily many 3–handles. We conclude with two classification results. The first shows that surfaces admitting doubly-standard shadow diagrams are unknotted. The second says that a b–bridge trisection in which some sector contains at least $b - 1$ patches is completely decomposable, thus the corresponding surface is unknotted. This settles affirmatively a conjecture of the second and fourth authors.

1 Introduction

One of the most important avenues available for studying in knotted surfaces in 4–space is the analysis of the 3–dimensional Seifert solids bounded by such surfaces. There are many situations in which information about such a Seifert solid gives rise to useful information about the corresponding knotted surface. Examples, ranging from classical to modern, include Gordon's proof that 2–knots are not determined by their complements [Gor76], Cochran's characterization of fibered, homotopy-ribbon 2-knots [Coc83], and recent work analyzing the relevance of homology cobordism invariants of Seifert solids [DM23].

In this paper, we show how topological information about a knotted surface can be recovered from a bridge trisection of the surface, which allows for the diagrammatic study of knotted surfaces and their Seifert solids. A *bridge trisection* of a surface $\mathcal{S}$ in S^4 is a certain decomposition of $(S^4, \mathcal{S})$ into three trivial disk systems $(B_1^4, \mathcal{D}_1), (B_2^4, \mathcal{D}_2), (B_3^4, \mathcal{D}_3)$ that can be encoded diagrammatically either as a triple of tangles called a *tri-plane diagram* or as a corresponding *shadow diagram*.

In Section 3, we give a version of Seifert's algorithm for bridge-trisected surfaces, showing how a tri-plane diagram can be used to produce a 3–manifold bounded by a connected surface $\mathcal{S}$ with normal Euler number zero.

Theorem 3.4 *If $\mathcal{S}$ is connected and $e(\mathcal{S}) = 0$, then there is a procedure to produce a Seifert solid for $\mathcal{S}$ that takes as input a tri-plane diagram for $\mathcal{S}$.*

In Subsection 3.2, we give an explicit procedure for constructing a Heegaard diagram for such a 3–manifold when $\mathcal{S} \cong S^2$. As a corollary of the work in building Seifert solids, we recover a combinatorial proof of the existence of Seifert solids. Although the literature already contains a method for producing a Heegaard diagram for a Seifert solid – namely, the work in [CS97] – the procedure described here is a bit more practical. In Section 3 of [CS97], the authors employ their methods to take a broken surface diagram and produce a genus 21 Heegaard diagram for a punctured $L(3, 1)\#\left(\#^3(S^1 \times S^2)\right)$ bounded by the 2-twist spun trefoil, noting that this solid is non-minimal, since the same 2-knot also bounds a punctured $L(3, 1)$. In contrast, in Subsection 3.3 we use our procedure to find genus three Heegaard diagrams for Seifert solids bounded by the spun trefoil and 1-twist spun trefoil, where these solids are minimal. For the 2-twist spun trefoil, the procedure yields a genus four Heegaard diagram for a Seifert solid (calculations omitted here). The 2-dimensional data contained in a tri-plane diagram can often be easier to manipulate and simplify than the data in a broken surface diagram; as such, both the solids and their Heegaard diagrams produced by Theorem 3.4 are likely to be less complicated.

We also show that certain bridge trisected surfaces are unknotted.

Theorem 3.3 *If a surface $\mathcal{S}$ has a doubly-standard shadow diagram, then $\mathcal{S}$ is unknotted.*

In practice, Theorem 3.3 offers a new and effective method to show unknottedness for bridge trisected surfaces. The doubly-standard criterion has considerable potential to aid in the tabulation of low-complexity knotted surfaces, since verifying that a shadow diagram is doubly-standard can be much easier than proving unknottedness via other methods.

One of the key features of trisection theory is that it provides a vehicle to adapt 3–dimensional ideas to dimension four, and in Section 4, we prove another result that fits into this line of research. It is well-known that the complement of every *canonical* Seifert surface (i.e. one obtained from Seifert's algorithm) is a handlebody. Thus, it is natural to attempt to extend this notion to dimension four. In this vein, we call a Seifert solid *canonical* if it is obtained from the procedure presented in Section 3, and we call a Seifert solid *spinal* if its exterior in S^4 can be built without 3–handles. We prove the following two results relating (and distinguishing) these concepts.

Theorem 4.1 *If a surface-knot $\mathcal{S}$ admits a Seifert solid, then it admits a canonical Seifert solid that is spinal.*

In fact, modulo some additional, easily satisfied connectivity conditions, every canonical Seifert solid is spinal. The next result shows that some Seifert solids (in contrast to canonical Seifert solids and many standard examples) are "far" from being spinal.

Theorem 4.2 *Given any $n \in \mathbb{N}$, there exists a 2–knot $\mathcal{K}$ that bounds a Seifert solid Y homeomorphic to $(S^1 \times S^2)^\circ$ such that $S^4 \setminus \nu(Y)$ requires at least n 4–dimensional 3–handles.*

Finally, in Section 5 we prove the following standardness result, affirmatively settling Conjecture 4.3 of [MZ17].

Theorem 5.2 *Let $\mathfrak{T}$ be a $(b; \mathbf{c})$–bridge trisection with $c_i = b - 1$ for some $i \in \mathbb{Z}_3$. Then, $\mathfrak{T}$ is completely decomposable, and the underlying surface-link is either the unlink of $\min\{c_i\}$ 2–spheres or the unlink of $\min\{c_i\}$ 2–spheres and one projective plane, depending on whether $|c_{i-1} - c_{i+1}| = 1$ or 0.*

The proof relies on theorems of Scharlemann and Bleiler-Scharlemann regarding planar surfaces in 3–manifolds [BS88, Sch85]. The methods of the proof are somewhat unrelated to the methods used in the preceding sections and may be of independent interest. The second and fourth authors previously handled this case when $c_i = b$ for some $i \in \mathbb{Z}_3$ [MZ17, Proposition 4.1]. Theorem 5.2 can be seen as the analogue for bridge trisections of Theorem 1.2 of [MSZ16], which establishes a similar standardness result for trisections of closed manifolds; as such, our theorem fills an important gap in the trisections literature and provides yet another avenue to verify that a surface in S^4 is unknotted.

Acknowledgements

2 Preliminaries

We work in the smooth category. This section includes an abbreviated introduction to the concepts relevant to this paper, but the interested reader is encouraged to consult the

reference [GK16] for further information about 4–manifold trisections and the references [MZ17] and [JMMZ22, Section 2] for more detailed discussions of bridge trisections. We limit our work here to surfaces in S^4, but there is also a theory of bridge trisections in arbitrary 4–manifolds; see [MZ18].

2.1 Bridge trisections

Let $\mathcal{S}$ be an embedded surface in S^4, let b be a positive integer, and let $\mathbf{c} = (c_1, c_2, c_3)$ be a triple of positive integers. A $(b; \mathbf{c})$–*bridge trisection* of $(S^4, \mathcal{S})$ is a decomposition

$$(S^4, \mathcal{S}) = (X_1, \mathcal{D}_1) \cup (X_2, \mathcal{D}_2) \cup (X_3, \mathcal{D}_3)$$

such that

(1) Each $\mathcal{D}_i$ is a collection of c_i boundary-parallel disks in the 4–ball X_i;

(2) Each intersection $\mathcal{T}_i = \mathcal{D}_{i-1} \cap \mathcal{D}_i$ a boundary-parallel tangle in the 3–ball $H_i = X_{i-1} \cap X_i$ (with indices considered mod 3);

(3) The triple intersection $\mathcal{D}_1 \cap \mathcal{D}_2 \cap \mathcal{D}_3$ is a collection of b points in the 2–sphere $\Sigma = X_1 \cap X_2 \cap X_3$.

In [MZ17], it was proved that every surface $\mathcal{S}$ admits a $(b; \mathbf{c})$–bridge trisection for some $(b; \mathbf{c})$. We choose orientations so that $\partial(X_i, \mathcal{D}_i) = (H_i, \mathcal{T}_i) \cup (\overline{H_{i+1}}, \overline{\mathcal{T}_{i+1}})$. When we wish to be succinct, we use $\mathfrak{T}$ to represent a bridge trisection, with components labeled as above.

2.2 Diagrams for bridge trisections

The existence of bridge trisections gives rise to a new diagrammatic theory for surfaces in S^4, using an object called a *tri-plane diagram*, a triple $\mathbb{D} = (\mathbb{D}_1, \mathbb{D}_2, \mathbb{D}_3)$ of trivial planar diagrams with the additional condition that each $\mathbb{D}_i \cup \overline{\mathbb{D}}_{i+1}$ is a classical diagram for an unlink. In [MZ17], it was shown that every tri-plane diagram determines a bridge trisection $\mathfrak{T}$. Conversely, given a bridge trisection $\mathfrak{T}$ of $(S^4, \mathcal{S})$, we can choose a triple of disks $E_i \subset H_i$ with common boundary and project the tangles $\mathcal{T}_i$ onto E_i to obtain a tri-plane diagram. Of course, the choices of disks and projections are not unique, but any two tri-plane diagrams corresponding the same bridge trisection $\mathfrak{T}$ are related by a finite collection of *interior Reidemeister moves* and *mutual braid transpositions*, while any two bridge trisections $\mathfrak{T}$ and $\mathfrak{T}'$ for the same surface $\mathcal{S}$ are related by *perturbation* and *deperturbation* moves.

In addition, bridge trisections yield another type of diagram: Each trivial tangle $\mathcal{T}_i$ can be isotoped rel-boundary into the surface Σ, yielding a triple (A, B, C) of pairwise disjoint collections of arcs called a *shadow diagram*, which has the property that $\partial A = \partial B = \partial C$, and the pairwise unions of any two of the tangles $\mathcal{T}_A$, $\mathcal{T}_B$, $\mathcal{T}_C$ determined by the arcs are

unlinks. As with tri-plane diagrams, any shadow diagram determines a bridge trisection. Further details about shadow diagrams can be found in [MTZ20].

Here we consider special types of shadow diagrams. We say that a pair of collections of arcs in a shadow diagram is *standard* if their union is embedded. Any bridge trisection admits a shadow diagram (A, B, C) in which one of the pairs is standard. If two or three pairs of shadows in a shadow diagram (A, B, C) are standard, then we say that (A, B, C) is *doubly-standard* or *triply-standard*, respectively. Theorem 3.3 says that doubly-standard (and thus triply-standard) diagrams always describe unknotted surfaces.

2.3 Unknotted surfaces

In this subsection, we review standard notions of unknottedness for surfaces in S^4. A closed, connected, orientable surface $\mathcal{S}$ in S^4 is *unknotted* if it bounds an embedded 3–dimensional handlebody $H \subset S^4$. For nonorientable surfaces, the definition is slightly more involved. We define the two unknotted projective planes, $P_\pm$, to be the two standard projective planes in S^4, pictured via their tri-plane diagrams in Figure 1, where $e(P_\pm) = \pm 2$.
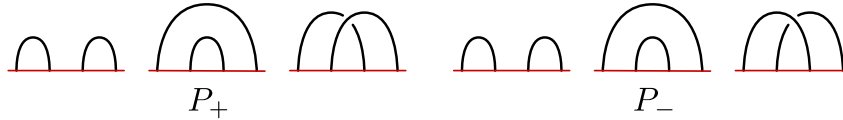

Figure 1: Tri-plane diagrams for P_+ and P_-.

In general, for a nonorientable surface $\mathcal{S}$, we say that $\mathcal{S}$ is *unknotted* if $\mathcal{S}$ is isotopic to a connected sum of some number of copies of P_+ and P_-. See [JMMZ22, Remark 2.6] for a detailed discussion of the orientation conventions used here.

3   Seifert solids

Classical results of Gluck [Glu62] (resp., Gordon-Litherland [GL78]) assert that every orientable surface $\mathcal{S}$ (resp., surface $\mathcal{S}$ with $e(\mathcal{S}) = 0$) in S^4 bounds an embedded 3–manifold, called a *Seifert solid* in the orientable case. In the setting of broken surface diagrams, Carter and Saito provided a procedure that in many respects mimics Seifert's algorithm for classical knots [CS97]. In this section, we describe an extension of Seifert's algorithm that takes an oriented tri-plane diagram $\mathbb{D}$ and produces a Seifert solid whose intersection with ∂X_i agrees with the classical Seifert's algorithm performed on the oriented unlink diagram $\mathbb{D}_i \cup \overline{\mathbb{D}}_{i+1}$. We also obtain alternative proofs of the theorems of Gluck and Gordon-Litherland mentioned above.

3.1   Existence of Seifert solids

Given a spanning surface F for an unlink U, we define the *cap-off* $\mathcal{F}$ of F to be the closed surface $\mathcal{F} \subset S^4$ obtained by gluing a collection of trivial disks in B^4_- to F along U. (There is a unique such choice of disks up to isotopy rel-boundary in B^4_- by e.g. [KSS82] or [Liv82].) Let $F_+ \subset S^3$ denote the Möbius band bounded by the unknot so that F_+ contains a positive half-twist and has boundary slope $+2$, and let $F_- \subset S^3$ denote the Möbius band bounded by the unknot with a negative half-twist and boundary slope -2. For $n > 0$, let F_n be the connected surface obtained by attaching $n - 1$ trivial bands to the split union of n copies of F_+; that is, F_n is obtained by taking the boundary connected sum of n copies of F_+. For $n < 0$, let F_n be obtain by taking the boundary connected sum of $(-n)$ copies of F_-. Finally, let F_0 be the disk bounded by the unknot in S^3. Additionally, let $\mathcal{F}_n$ be the cap-off of F_n. In Figure 1, the negative Möbius band is shown to cap off into B^4_+ to obtain P_+. (See also [JMMZ22, Figure 2].) Here, we are capping off into B^4_-, so that by definition the cap-off $\mathcal{F}_{-1}$ of the negative Möbius band F_- is P_-. In contrast, the cap-off $\mathcal{F}_1$ of the positive Möbius band F_+ is P_+. (Recall that P_+ and P_- denote the two unknotted projective planes in S^4; see Subsection 2.3.) It follows that

$$
\mathcal{F}_n = \begin{cases} \text{a connected sum of } n \text{ copies of } P_+, & \text{if } n > 0 \\ \text{a connected sum of } -n \text{ copies of } P_- & \text{if } n < 0 \, , \\ \text{an unknotted 2–sphere} & \text{if } n = 0 \end{cases}
$$

The intent of the cap-off notation is to emphasize the way in which $\mathcal{F}_n$ can be obtained from a specific surface in S^3, which will be useful in the rest of this section – especially given the following lemma.

Lemma 3.1 *Every incompressible spanning surface F for the unknot is isotopic to F_n for some $n \in \mathbb{Z}$.*

Proof First, we argue that F_n is incompressible for all n. This follows from [Tsa92], but we include a proof here. Certainly, F_0 and $F_{\pm 1}$ are incompressible, since a compression increases Euler characteristic by two. Suppose now that F_n is compressible for some $n > 1$, and let F'_n be the component of the surface obtained by compressing F_n such that $\partial F'_n = \partial F_n$. In addition, let $\mathcal{F}'_n \subset S^4$ be the cap-off of F'_n. Then the embedded surface $\mathcal{F}_n$ can be obtained from $\mathcal{F}'_n$ by a 1–handle attachment, and thus $e(\mathcal{F}'_n) = e(\mathcal{F}_n) = 2n$. However, since the nonorientable genus of $\mathcal{F}'_n$ is strictly less than n, this contradicts the Whitney–Massey Theorem (see discussion in [JMMZ22]). We conclude that F_n is incompressible.

On the other hand, suppose that F is an arbitrary incompressible spanning surface for the unknot U. The exterior of U is a solid torus V, and every simple closed curve $c \subset \partial V$ is homotopic to a (p, q)–curve, where a $(0, 1)$–curve is the boundary of a meridian disk of

V and a $(1,0)$–curve is the boundary of a meridian disk of $N(U)$. The boundary of F is a $(2k, 1)$–curve for some integer k. (The spanning surface F intersects the disk bounded by U in some number of arcs, the endpoints of which correspond to the intersections of the (p, q)–curve with the $(0, 1)$–curve.) If F is orientable, then it is well-known that F is isotopic to the meridian disk F_0.

Suppose that F is nonorientable. By [Tsa92, Corollary 12], the nonorientable genus of F is equal to $|k|$. Assuming that ∂F and ∂F_0 meet efficiently, isotope F so that it intersects F_0 minimally. By standard cut-and-paste arguments, an arc of $F \cap F_0$ which is outermost in F_0 gives rise to a boundary-compressing disk Δ for F. Since ∂F and ∂F_0 meet efficiently, the result F' of boundary-compressing F along Δ has a single boundary component and nonorientable genus $k - 1$. Reversing the process, we see that F can be obtained from F' by attaching a boundary-parallel band to F' along opposite sides of $\partial F'$. Note that $\partial V \setminus \partial F'$ is an annulus and the band is determined by a spanning arc. Working rel-boundary, all choices of spanning arcs are related by Dehn twists about $\partial F'$, and so it follows that up to isotopy, there is a unique band taking F' to F.

Finally, we claim that F is isotopic to F_k, and we prove this fact by inducting on k. If $k = \pm 1$, then F has genus one and is obtained from the disk $F' = F_0$ by a single boundary tubing. By the above argument, there is precisely one way to do this, and thus $F = F_{\pm 1}$. Now, suppose that $k > 1$ and the claim holds for $j = k - 1$. As above, isotope F to meet F_0 minimally, and since $k > 1$, there are at least two arcs a_0 and a_1 of $F \cap F_0$ that are outermost in F_0. Let ℓ be a $(0, 1)$-curve that meets ∂F in a single point contained in a_0. Then, a_1 gives rise to a boundary-compressing disk Δ_1 and the result F' of boundary-compressing F along Δ_1 also satisfies $|\partial F' \cap \ell| = 1$, since the modification was carried out away from the arc a_0. We conclude that F' has genus $k - 1$ and boundary slope $(2(k - 1), 1)$. By induction $F' = F_{k-1}$, and since there is a unique way to obtain F from F' by boundary-tubing, it follows that $F = F_k$. The case $k < -1$ follows symmetrically, completing the proof of the lemma. $\square$

In the next proposition, we use Lemma 3.1 to understand the cap-off of any spanning surface F for an unlink in S^3.

Proposition 3.2 *Let F be a spanning surface for an unlink U in S^3.*

(1) *If every component of ∂F has slope 0, then the cap-off $\mathcal{F}$ bounds a (possibly nonorientable, possibly disconnected) handlebody $V \subset B^4$ such that $V \cap \partial B^4 = F$.*

(2) *The normal Euler number $e(\mathcal{F})$ is equal to the sum of the slopes of the boundary components of F.*

(3) *The cap-off $\mathcal{F}$ is a split union of unknotted surfaces in S^4.*

Proof Suppose F and F' are two spanning surfaces for an unlink U in S^3 such that F' is isotopic relative to U to the surface obtained by surgering F along a compressing disk D for F. Then there is a compression body $C \subset S^3 \times [0, 1]$ such that

- $C \cap (S^3 \times \{1\}) = F \times \{1\}$,
- $C \cap (S^3 \times \{0\}) = F' \times \{0\}$, and
- $\partial C = (F \times \{1\}) \cup (\overline{F' \times \{0\}}) \cup (U \times [0, 1])$,

and C has a single critical point (of index 1) with respect to the Morse function $S^3 \times [0, 1] \to [0, 1]$, which we assume lies in $S^3 \times \{\frac{1}{2}\}$. Note that C is a product cobordism above and below $S^3 \times \{\frac{1}{2}\}$.

Any spanning surface F for U can be reduced to F', a union of 2–spheres and incompressible spanning surfaces for components of U via a sequence of compressions and isotopies. If each component of ∂F has slope 0, then F' is a collection of disks and spheres. Applying the compression body construction described above for each compression taking F to F' and stacking the results, we get a compression body C co-bounded by F and F'. Since F' is a collection of disks and spheres, there is a handlebody with boundary $\mathcal{F} = F \cup \mathcal{D}$, where $\mathcal{D} = \overline{F'} \cup (U \times [0, 1])$ is a collection of properly embedded disks in B^4: simply cap-off the sphere components of C with 3–balls whose interiors are pushed sufficiently deep into B^4. This handlebody is non-orientable (resp., disconnected) if and only if F is. This establishes part (1).

Let F be any spanning surface for an unlink $U = \bigsqcup_{i=1}^{n} U_i$. Let $B = \bigsqcup_{i=1}^{n} B_i$ be a collection of disjoint 3–balls with $U_i \subset \text{Int}(B_i)$. Let $F' = \bigsqcup_{i=1}^{n} F_i$ be a split union of incompressible spanning surfaces for the components of U, with $F_i \subset \text{Int}(B_i)$, so that the slopes of F and F' agree at each component of U. Let F'' be the result of surgering F' along a collection of arcs so that F'' and F have the same homeomorphism type relative to U; moreover, assume that every arc of the collection intersects each component of ∂B in at most one point. It follows that F'' decomposes as a split union of connected sums of surfaces, each summand of which is either a torus or an incompressible spanning surface for an unknot. Therefore, the cap-off $\mathcal{F}''$ is the split union of connected sums of surfaces, each summand of which is an unknotted surface in S^4. Livingston showed that F and F'' are isotopic rel-boundary in B^4 [Liv82]. It follows that the cap-off $\mathcal{F}$ will isotopic to the cap-off $\mathcal{F}''$, which completes the proof of part (3). Since (2) holds for $\mathcal{F}_1$ and $\mathcal{F}_{-1}$, and since the normal Euler number is additive under connected sum, part (2) follows, as well. □

Recall that a shadow diagram is doubly-standard if two of the pairings of arcs yield embedded curves. We can use Proposition 3.2 to obtain the following classification result for doubly-standard diagrams.

Theorem 3.3 *If $\mathcal{S}$ has a doubly-standard shadow diagram, then $\mathcal{S}$ is unknotted.*

Note that Theorem 3.3 also applies to surfaces with triply-standard shadow diagrams, as a special class of doubly-standard shadow diagrams.

Proof Suppose $\mathcal{S}$ has a shadow diagram (A, B, C) such that the pairings (A, B) and (B, C) are standard. Consider the standard Heegaard splitting $\partial X_3 = S^3 = H_+ \cup_\Sigma H_-$, and let $\Sigma_\pm$ be a parallel copy of Σ pushed slightly into $H_\pm$. Note that $A \cup B$ may have nested components (so that components of $A \cup B$ don't necessarily bound a collection of disjoint disks). After a sequence of arc slides, however, performed only on the arcs in A, we obtain arcs A' such that the embedded curves $A' \cup B$ bound a pairwise disjoint collection of disks. We perform a similar procedure with $B \cup C$ to obtain $B \cup C'$. Now, embed parallel copies $A'_+ \cup B_+$ of the curves $A' \cup B$ in Σ_+ so that they bound a pairwise disjoint collection D_+ of disks in Σ_+, and embed parallel copies $B_- \cup C'_-$ of the curves $B \cup C'$ in Σ_- so that they bound a pairwise disjoint collection D_- of disks in Σ_-. In H_+, there is an isotopy of B_+ to $B \subset \Sigma$ taking the disks D_+ to disks $D_1 \subset H_+$ such that $D_1 \cap \Sigma = B$. The tangle $\mathcal{T}_1 = \mathcal{S} \cap (H_+)$ is the image of A'_+ under this isotopy. Similarly, in H_- there is an isotopy of B_- to B taking the disks D_- to disks $D_2 \subset H_-$ such that $D_2 \cap \Sigma = B$. The tangle $\mathcal{T}_3 = \mathcal{S} \cap H_-$ is the image of C'_- under this isotopy. See Figure 2.

By construction $D_1 \cap D_2 = B$, so that $F = D_1 \cup D_2$ is a spanning surface for the unlink $\mathcal{T}_1 \cup \mathcal{T}_3$. Note further that D_1 is a trivial disk system for $\mathcal{T}_1 \cup B$, and D_2 is a trivial disk system for $B \cup \mathcal{T}_3$; hence, $\mathcal{S}$ is the union of D_1, D_2, and D_3, where D_3 is a trivial disk system for $\mathcal{T}_1 \cup \mathcal{T}_3$ pushed into B^4. However, since $F = D_1 \cup D_2 \subset S^3$, it follows that $\mathcal{S}$ is also isotopic to the cap-off $\mathcal{F}$ of F, which is unknotted by Proposition 3.2. $\square$

We are now ready to prove our main result.

Theorem 3.4 *If $\mathcal{S}$ is connected and $e(\mathcal{S}) = 0$, then there is a procedure to produce a Seifert solid for $\mathcal{S}$ that takes as input a tri-plane diagram for $\mathcal{S}$.*

Proof The proof follows from the proofs of Propositions 3.5 and 3.6 below. $\square$

In Section 3.2, we show that there is a procedure to produce a Heegaard splitting for the Seifert solid when $\mathcal{S}$ is a 2–knot.

In addition to providing the proof of the above theorem, the next two propositions provide alternate proofs of the results in [Glu62] and [GL78] mentioned above.

Proposition 3.5 *Every orientable surface-link $\mathcal{S}$ bounds a Seifert solid in S^4.*

Proof Let $\mathbb{D}$ be a tri-plane diagram for $\mathcal{S}$, with induced orientation on the bridge points **x**. Perform mutual braid transpositions so that the bridge points alternate sign (orientation).
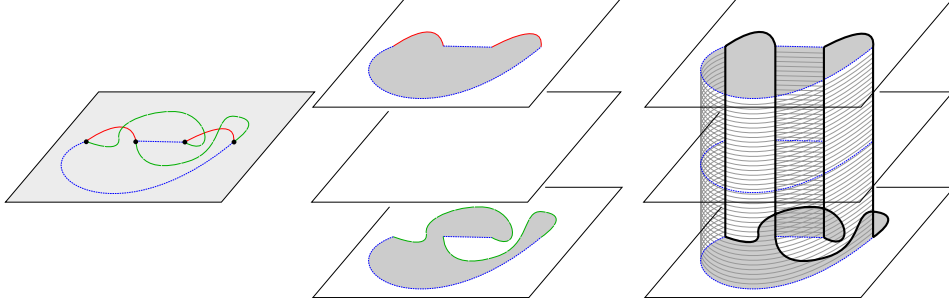
Figure 2: Left: a doubly standard shadow diagram (A, B, C). The pairings (A, B) and (B, C) are standard. Middle: disks in Σ_+ and Σ_- bounded by parallel copies of $A \cup B$ and $B \cup C$, respectively. Right: A spanning surface F for $\mathcal{T}_1 \cup \mathcal{T}_2$ in $\partial X_3 = S^3$.

Then there are b pairwise disjoint arcs ε contained in the equator e connecting bridge points of opposite signs, so that $\mathbb{D}_i \cup \varepsilon$ is an oriented link diagram. Let F_i be the Seifert surface obtained by performing Seifert's procedure on the diagram $\mathbb{D}_i \cup \varepsilon$, and let $\widehat{F}_i = F_i \cup \overline{F}_{i+1}$ be the spanning surface obtained by gluing F_i to $\overline{F}_{i+1}$ along ε. By Proposition 3.2, there exists a handlebody $V_i \subset X_i$ such that $\partial V_i = \widehat{F}_i \cup \mathcal{D}_i$ and $V_i \cap \partial X_i = \widehat{F}_i$. Finally, $Y = V_1 \cup V_2 \cup V_3$ is an embedded 3–manifold whose boundary is $\mathcal{D}_1 \cup \mathcal{D}_2 \cup D_3 = S$, and so Y is a Seifert solid for $\mathcal{S}$. $\qquad\square$

Proposition 3.6 *If $\mathcal{S}$ is connected and $e(\mathcal{S}) = 0$, then $\mathcal{S}$ bounds a spanning solid in S^4.*

Proof Consider a bridge trisection $\mathfrak{T}$ of $\mathcal{S}$, with $U_i = \partial \mathcal{D}_i$ and $\tau = \mathcal{T}_1 \cup \mathcal{T}_2 \cup \mathcal{T}_3$. By taking, for example, a tri-plane diagram $\mathbb{D}$ and compatible checkerboard surfaces in $\mathbb{D}_i$, we can produce spanning surfaces $\widehat{F}_i$ for U_i such that $\widehat{F}_i \cap H_i = \widehat{F}_{i-1} \cap H_i$. Let F_i denote $\widehat{F}_i \cap H_i$. For each component J of $U_i = \partial \widehat{F}_i$, let $\iota_{\widehat{F}}(J)$ denote the induced boundary slope on the curve J by the surface $\widehat{F}_i$. Then by Proposition 3.2, we have

$$\sum_{J \subset U_1 \cup U_2 \cup U_3} \iota_{\widehat{F}}(J) = 0.$$

Choose a triple of spanning surfaces $\widehat{F}_i$ such that $\sum |\iota_{\widehat{F}}(J)|$ is minimal over all possible choices. We claim that $\sum |\iota_{\widehat{F}}(J)| = 0$. If not, then there exist boundary curves J_+ and J_- such that $\iota_{\widehat{F}}(J_+) > 0$ and $\iota_{\widehat{F}}(J_-) < 0$. Noting that the surface $\mathcal{S}$ contains all curves $J \subset U_i \subset \tau$, push each curve $J \subset U_i$ slightly off of τ into the corresponding disk component of $\mathcal{D}_i$, so that the collection of curves J is embedded in $\mathcal{S}$ and disjoint from τ. Choose a path $\gamma \subset \mathcal{S}$ from J_+ to J_-, avoiding the bridge points, noting that $|\gamma \cap \tau| > 0$. At each point of $\gamma \cap \tau$, modify the the corresponding component of F_i by taking the boundary connected sum of F_i with a trivial Möbius band to obtain new surfaces $\widehat{F}'_i$ and F'_i, so that the corresponding boundary curves satisfy $\iota_{\widehat{F}'}(J'_+) = \iota_{\widehat{F}}(J_+) - 2$, $\iota_{\widehat{F}'}(J'_-) = \iota_{\widehat{F}}(J_-) + 2$, and

$\iota_{\widehat{F}'}(J') = \iota_{\widehat{F}}(J)$ for all other curves J'. It follows that $\sum |\iota_{\widehat{F}'}(J')| < \sum |\iota_{\widehat{F}}(J)|$, contradicting our assumption of minimality. (Note that $\iota_{\widehat{F}}(J)$ is always even, since it represents the number of intersection points between the boundary curves of spanning surfaces; see the proof of Lemma 3.1.)

We conclude that $\iota_{\widehat{F}}(J) = 0$ for all curves J, and thus by Proposition 3.2, each spanning surface $\widehat{F}_i$ cobounds a (possibly) nonorientable handlebody $V_i \subset X_i$ with the disks $\mathcal{D}_i$. It follows that $V_1 \cup V_2 \cup V_3$ is a spanning solid for $\mathcal{S}$ in S^4. $\qquad\qquad\square$

3.2 Procedure to find a Heegaard diagram for a Seifert solid

In this subsection, we describe a procedure for finding a Heegaard diagram for the Seifert solid coming from a bridge trisection $\mathfrak{T}$ of a 2–knot $\mathcal{S}$. We use labels consistent with those appearing above in the proof of Proposition 3.5. The process is illustrated in Figures 3 through 6.

Step 1: Given a tri-plane diagram $\mathbb{D}$ for $\mathcal{S}$ perform interior Reidemeister moves and mutual braid transpositions so that the induced Seifert surfaces satisfy the following conditions:

   (a) Each of F_1, F_2, and $\widehat{F}_1$ is a collection of disks.

   (b) Surfaces $\widehat{F}_2$ and $\widehat{F}_3$ are connected.

   (c) $g(\widehat{F}_2) = g(F_3)$.

See Figure 3. Note that attaining condition (a) is possible since any tri-plane diagram can be converted to one in which two of the tangles have no crossings. Condition (b) can be attained by performing interior Reidemeister moves on the diagram $\mathbb{D}_3$. Attaining condition (c) is possible since we can arrange so that F_2 is a collection of b bridge disks, in which case $\widehat{F}_2$ deformation retracts onto F_3 (although in general, we need not assume that F_2 has b components, as shown below).

Step 2: Following the proof of Proposition 3.2, the surfaces $\widehat{F}_2$ and $\widehat{F}_3$ compress completely to disks in S^3. Let α be a complete collection of pairwise disjoint compressing curves in $\widehat{F}_3$, and let β be a complete collection of pairwise disjoint compressing curves in $\widehat{F}_2$. See Figure 4 (top row).

Step 3: If necessary, slide the curves β over the components of $\partial \mathcal{D}_2$ to obtain a collection of curves $\beta' \subset F_3$. Note that since $g(F_3) = g(\widehat{F}_2)$, as curves in $\mathcal{F}_2 = \widehat{F}_2 \cup \mathcal{D}_2$, the collection β can be isotoped to be contained in F_3, and any isotopy of a curve over a disk component of $\mathcal{D}_2$ can be realized as a slide over $\partial \mathcal{D}_2$. Thus, such a sequence of slides exists. See Figure 4 (middle row).

Step 4: Let $P = \mathcal{D}_1 \cup \mathcal{D}_2$, so that P is a planar surface with c_3 boundary components, let Q be the surface obtained by gluing P to $\widehat{F}_3$ along their boundaries, and let α^* be a choice

Figure 3: To perform the Seifert solid procedure on a tri-plane diagram, we first perform mutual braid transposition until the tangle diagrams in V_1 and V_2 have no crossings. Then we perform the usual Seifert's procedure for knot diagrams to obtain surfaces F_1, F_2, F_3 that agree in the bridge sphere Σ, with F_1 and F_2 and $\widehat{F}_1$ all collections of disks and $g(\widehat{F}_2) = g(F_3)$.

of $c_3 - 1$ boundary components of P and some minimal number of curves in α so that α^* forms a cut system for Q.

Step 5: Let β^* be the union of β' and a collection of curves in Q obtained by the following instructions: For each component of J of $\partial \mathcal{D}_1$, suppose that J meets d disk components of F_2. Choose $d - 1$ of these components, isotope them off of F_2 in $\mathcal{F}_2 = F_2 \cup F_3 \cup \mathcal{D}_2$, and add these $d - 1$ curves to β^*. Discard any superfluous curves of β' so that β^* is a cut system for Q.

Proposition 3.7 *Using the procedure described above, $\mathcal{S}$ bounds a punctured copy of the 3–manifold determined by the Heegaard diagram $(Q; \alpha^*, \beta^*)$.*

Proof Suppose that $\mathbb{D}$ is a tri-plane diagram satisfying conditions (a), (b), and (c) given in Step 1 above. Following the proofs of Proposition 3.2 and Proposition 3.5, we have
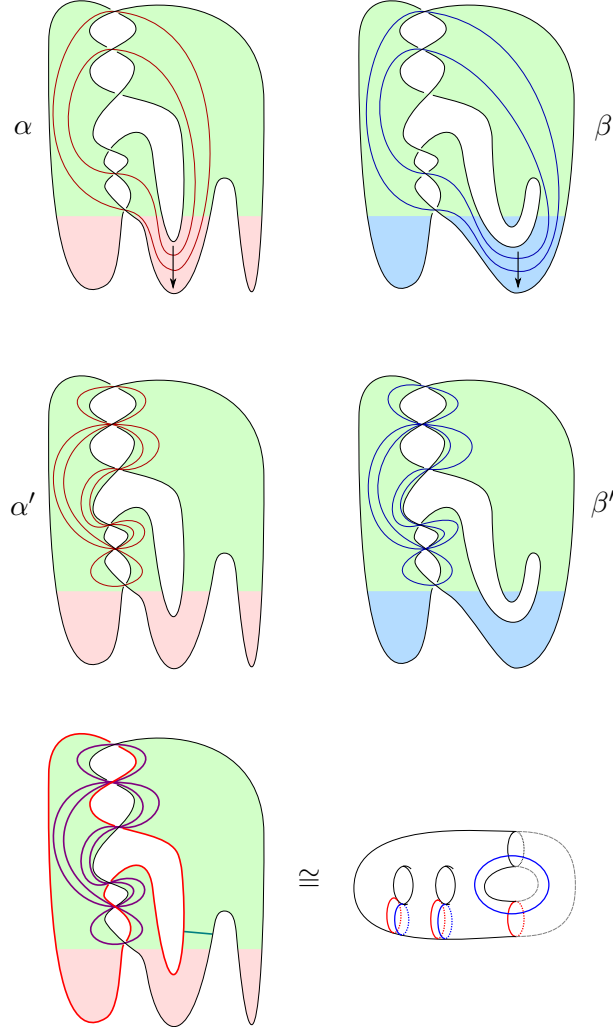
Figure 4: Top: we find complete sets of compressing curves α, β for $\widehat{F}_3$ and $\widehat{F}_2$, respectively. Middle: We slide α, β (with slides indicated in top row) over $\partial\widehat{F}_3, \partial\widehat{F}_2$ to obtain curve systems α', β' that are each completely within F_3. Bottom: We obtain α^* (red and purple curves) by adding boundary curves as in Step (4) of §3.2. We obtain β^* by adding arcs as in Step (5). Then $(Q; \alpha^*, \beta^*)$ is a Heegaard diagram for a (closure of a) Seifert solid for the 2–knot described by the initial tri-plane diagram.

that for each i, the surface $\widehat{F}_i \cup \mathcal{D}_i$ bounds a handlebody V_i, where V_1 is a collection of 3–balls, say $B_1, \ldots, B_n$, and V_2 and V_3 are connected. Moreover, α contains a cut system for V_3 and β contains a cut system for V_2. Since β' is homotopic to β in ∂V_2, it follows that β' also contains a cut system for V_2. Thus, the Seifert solid bounded by $\mathcal{S}$ is equal to $V_2 \cup V_3 \cup B_1 \cup \cdots \cup B_n$. Let Y be the closed 3–manifold obtained by capping off the
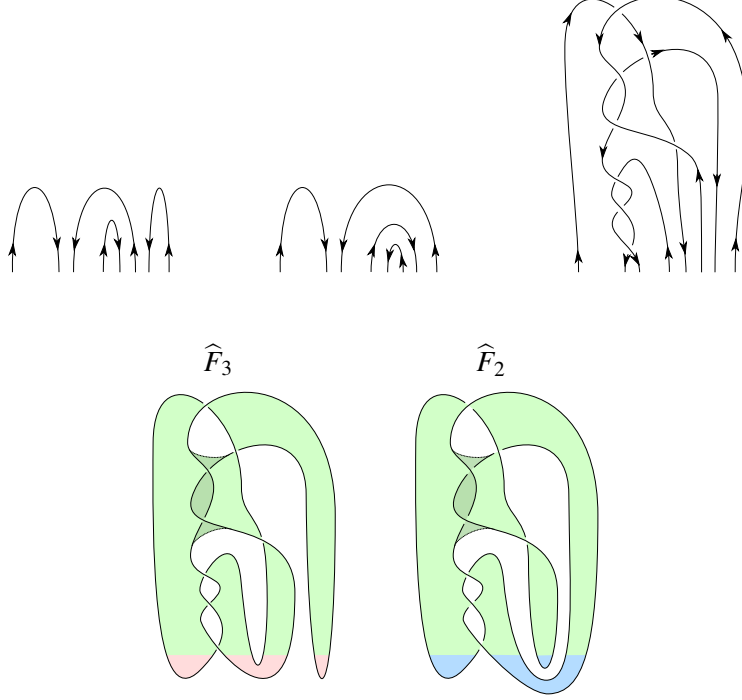
Figure 5: We start performing the Seifert solid procedure (§3.2) on the tri-plane diagram in the top row.

boundary $\mathcal{S}$ of this Seifert solid with an abstract 3–ball B_0. We will show that $(Q; \alpha^*, \beta^*)$ is a Heegaard diagram for Y.

To this end, consider $W = V_3 \cup B_0$ and $W' = V_2 \cup B_1 \cup \cdots \cup B_n$. Considering that $\partial V_2 = F_2 \cup F_3 \cup \mathcal{D}_2$ and $\partial(B_1 \cup \cdots \cup B_n) = F_1 \cup F_2 \cup \mathcal{D}_1$, we have that

$$\partial W' = F_3 \cup F_1 \cup \mathcal{D}_2 \cup \mathcal{D}_1 = \widehat{F}_3 \cup P = Q.$$

Additionally, the 3–balls B_i are attached to V_2 along F_2, which is a collection of disks by condition (a). It follows that the curves $\beta' \cup \partial F_2$ bound compressing disks in W' cutting W' into a collection of 3–balls, so W' is a handlebody. In addition, choosing all but one curve of ∂F_2 for each component B_i and a subset of β' as in Step 5 above yields a cut system β^* for W'.

Turning our attention to W, we have $\partial V_3 = \widehat{F}_3 \cup \mathcal{D}_3$ and $\partial B_0 = \mathcal{D}_1 \cup \mathcal{D}_2 \cup \mathcal{D}_3$, so that $\partial W = \widehat{F}_3 \cup \mathcal{D}_1 \cup \mathcal{D}_2 = Q$, and in addition, the curves α and $\partial \mathcal{D}_3$ bound disks cutting W into 3–balls. Choosing α^* to contain all but one curve of $\partial \mathcal{D}_3$ and a subset of α as in Step 4, we have that the curves in α^* bound disks cutting W into a single 3–ball, so α^* is a cut system for W. We conclude that $(Q; \alpha^*, \beta^*)$ is a Heegaard diagram for Y, as desired.   □

Remark 3.8 It may be the case that the surface F_3 compresses in H_3, in which case α and

β could have one or more curves in F_3 in common. Following the procedure with such α and β produces one or more extra $S^1 \times S^2$ summands for the 3–manifold Y, and a simpler Seifert solid can be obtained by first compressing F_3 maximally in H_3.

Remark 3.9 The procedure above can be generalized: We can relax conditions (a), (b), and (c) from Step 1; the only assumption necessary to ensure that $V_1 \cup V_2$ is a handlebody is that their intersection F_2 is a collection of disks. However, the weaker conditions make it somewhat more difficult to draw the diagram, since we are no longer guaranteed the existence of the slides of Step 3 – it may be the case that β curves necessarily intersect the disks $\mathcal{D}_1$ and $\mathcal{D}_2$.

Remark 3.10 The observant reader might notice that we call our process the Seifert solid *procedure*, rather than *algorithm*. An algorithm gives an output completely determined from the input, independent of further choices. A procedure may require additional choices for the output to be determined. In the procedure we give in this section to find a description of a Seifert solid for a 2–knot, we are forced to choose compressing circles for surfaces in S^3. These circles are generally not unique (and in fact, different choices can determine different Seifert solids), so we do not refer to this procedure as an algorithm.

3.3 Some examples

In this subsection, we carry out the procedure described above for a couple of specific examples. The first is the spun trefoil. In Figure 3, we see a tri-plane diagram for the spun trefoil coming from [MZ17], followed by the result of performing tri-plane moves so that the induced Seifert surfaces F_i satisfy conditions (a), (b), and (c) from Step 1 above.
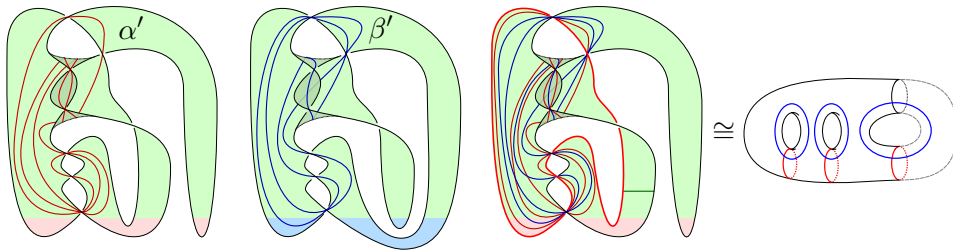

Figure 6: Leftmost: The curves α' in F_3. Second: The curves β' in F_2. Third: we add some boundary curves of F_2 to α to obtain α^* and some arc to β' to obtain β^*. Rightmost: we simplify the resulting Heegaard diagram $(\Sigma; \alpha^*, \beta^*)$ to see that it is a diagram of S^3. Thus, the initial 2–knot bounds a copy of B^3 in S^4, so is unknotted.

In the top panel of Figure 4, we find the compressing curves α on $\widehat{F}_3$ and β on $\widehat{F}_2$. Note that in this case $\mathcal{D}_3$ contains two disks, so that $P = \mathcal{D}_1 \cup \mathcal{D}_2$ is an annulus, and $Q = \widehat{F}_3 \cup P$ can

be obtained by identifying the two boundary components of $\widehat{F}_3$. Under this identification, the identified boundary components constitute the third curve in the cut system α^*. In the second panel at left, we slide the two curves of α over the third curve of α^* in Q. In the second panel at right, we slide the two curves of β over a boundary component as shown to get the curves $\beta' \subset F_3$ (which are identical to the image of α under the slides described above). Finally, the third curve of β^* consists of the teal arc depicted in F_3 and a spanning arc in the annulus A, or equivalently, we can identify the endpoints of the teal arc. In the lower panel, we see the diagram for the Seifert solid, the standard (once-stabilized) Heegaard diagram for $\#^2(S^1 \times S^2)$.

Remark 3.11 These diagrams and arguments easily generalize to produce the Seifert solid $\#^{p-1}(S^1 \times S^2)$ for the spun $(p, 2)$-torus knot. Miyazaki proved that the degree of the Alexander polynomial (over $\mathbb{Q}[t, t^{-1}]$) is a lower bound for the second Betti number of any Seifert solid [Miy86]. Since the degree of the Alexander polynomial of $T(2, p)$ is $p - 1$, these solids are minimal in the sense that the corresponding 2–knots cannot bound any 3-manifold with a smaller second Betti number, e.g. a fewer number of $S^1 \times S^2$ summands.

For the second example, we find a Seifert solid for the 1-twist spun trefoil (which is unknotted by [Zee65]). In Figure 5, we include a simplified tri-plane diagram for the 1-twist spun trefoil along with the surfaces $\widehat{F}_2$ and $\widehat{F}_3$ this diagram generates.

Next, we find the compressing curves α for $\widehat{F}_3$ and β for $\widehat{F}_2$. As in the spun trefoil example above, $P = \mathcal{D}_1 \cup \mathcal{D}_2$ is an annulus, so we view Q as being obtained by identifying the two boundary components of $\widehat{F}_3$, with this identified boundary the third curve in α^*. Figure 6 shows the curves α, β, and the union of the sets in Q, yielding the standard diagram for S^3, in which the third curve of β^* appears as a teal arc with boundary points identified (as above). Note that the existence of the curves α and β is guaranteed by Proposition 3.2; in practice, however, these curves are found using ad hoc methods.

4   Spinal Seifert solids

A natural aspect of the study of Seifert surfaces for links in the 3–sphere is the consideration of their exteriors. We call a Seifert surface F for L *canonical* if it is isotopic to a surface obtained by applying Seifert's procedure to a diagram for L. We call a Seifert surface F *free* if its exterior $S^3 \setminus \nu(F)$ is a 3–dimensional handlebody – equivalently, has free fundamental group. It is an easy exercise to see that a canonical Seifert surface is free, provided that it is connected; so every link admits a free Seifert surface, by the application of Seifert's algorithm to a non-split diagram. However, such a surface can be far from minimal genus. M. Kobayashi and T. Kobayashi showed that the difference between the genus of a knot and the minimal genus of a free Seifert surface for the knot can be arbitrarily large, and that

moreover the difference between the minimal genus of a free Seifert surface for a knot and the minimal genus of a canonical Seifert surface can also be arbitrarily large [KK96]. (In fact, they show that both of these differences can be made arbitrarily large at the same time.)

In this section, we introduce 4–dimensional analogues of the notions of canonical and free Seifert surfaces. Going forward, let $\mathcal{S} \subset S^4$ be a surface-link admitting a Seifert solid. (This is equivalent to the condition that $\mathcal{S}$ be orientable or have normal Euler number zero.) We call a Seifert solid Y *canonical* if it is isotopic to a Seifert solid obtained by the procedure given in Section 3.1 (see Propositions 3.5 and 3.6). We call a Seifert solid Y *spinal* if $S^4 \setminus \nu(Y)$ deformation retracts onto a finite 2–complex. Equivalently, $S^4 \setminus \nu(Y)$ can be built with handles of index at most two.

Theorem 4.1 *If a surface-knot $\mathcal{S}$ admits a Seifert solid, then it admits a canonical Seifert solid that is spinal.*

Proof First, note that in the proof of Propositions 3.5 and 3.6, it is possible to arrange that each Seifert surface F_i is connected: For example, this is assured if each $\mathbb{D}_i \cup \varepsilon$ is non-split. Let Y be a canonical Seifert solid for $\mathcal{S}$ given by Proposition 3.5 or Proposition 3.6 such that the canonical surface $F_i = Y \cap H_i$ is connected for each $i \in \mathbb{Z}_3$. We make use of the notation of the proof of Proposition 3.5 in what follows.

Recall that $V_i = X_i \cap Y$ is a handlebody with $\partial V_i = \widehat{F}_i \cup \mathcal{D}_i$. Moreover, V_i is built relative to $\widehat{F}_i$ by attaching 3–dimensional 2–handles and 3–handles. It follows that $X_i \setminus \nu(V_i)$ can be built with 4–dimensional 0–, 1–, and 2–handles.

Next, recall that F_i is a canonical Seifert surface for the link $\mathbb{D}_i \cup \varepsilon$, considered in $S^3 = H_i \cup_\Sigma B^3$. Since we have assumed F_i is connected, we have that F_i is free in $H_i \cup_\Sigma B^3$. Since $\varepsilon \subset \partial H_i$, it follows that $H_i \setminus F_i$ is also a 3–dimensional handlebody.

Finally, we can build $S^4 \setminus \nu(Y)$ by taking the $X_i \setminus \nu(V_i)$ and gluing them along the $H_i \setminus \nu(F_i)$. Since the three gluings occur along 3–dimensional handlebodies, it follows that $S^4 \setminus \nu(Y)$ is obtained from the disjoint union of the $X_i \setminus \nu(V_i)$ by attaching 4–dimensional 1– and 2–handles. Because each of the $X_i \setminus \nu(V_i)$ were built with 4–dimensional handles of index at most two, the same is true for $S^4 \setminus \nu(Y)$. This shows that Y is spinal, as desired. □

When studying Seifert surfaces, the genus of the surface is the obvious measure of complexity that one might try to minimize. In contrast, there are many ways one might try to quantify the complexity of a Seifert solid Y for a surface-knot; indeed, any complexity one might associate to a 3–manifold could be interesting to consider. Here, we content ourselves to give some examples showing that there is at least one sense in which a simple Seifert solid for a surface-knot can be arbitrarily far from being spinal.

Theorem 4.2 *Given any $n \in \mathbb{N}$, there exists a 2–knot $\mathcal{K}$ that bounds a Seifert solid Y homeomorphic to $(S^1 \times S^2)^\circ$ such that $S^4 \setminus \nu(Y)$ requires at least n 4–dimensional 3–handles.*

Proof Let J be an arbitrary knot, and let $K = \mathrm{Wh}_0(J \# \bar{J})$ be the untwisted Whitehead double of the connected sum of J with its mirror. Let F be the standard genus one Seifert surface for K, and let γ be the curve on F that is isotopic to $J \# \bar{J}$. (Alternatively, F is obtained by taking a 0–framed annular thickening of a curve γ isotopic to $J \# \bar{J}$ and plumbing on a Hopf band.)

Let E be the standard ribbon disk for γ, so that $(B^4, E) = (S^3, J)^\circ \times I$. The surface F can be surgered along E in the 4–ball to get a slice disk D for K, and the trace of this surgery yields a solid torus V with $\partial V = F \cup D$.

Let $\mathcal{K} = D \cup_K \bar{D}$ be the 2–knot obtained by doubling D, and let $Y = V \cup_F \bar{V}$ be the double of V along F. Then, Y is a Seifert solid for $\mathcal{K}$ and $Y \cong (S^1 \times S^2)^\circ$.

We claim that $\pi_1(S^4 \setminus \nu(Y)) \cong \pi_1(S^3 \setminus \nu(J))$. First, we have $\pi_1(S^4 \setminus \nu(Y)) \cong \pi_1(B^4 \setminus V)$, since the former exterior is the double of the latter exterior along the exterior of F in S^3 and $\pi_1(S^3 \setminus \nu(F))$ surjects onto $\pi_1(B^4 \setminus V)$ under inclusion. Next, by construction, V is obtained by thickening the slice disk E and attaching a trivial 3–dimensional 1–handle. It follows that

$$\pi_1(B^4 \setminus \nu(V)) \cong \pi_1(B^4 \setminus \nu(E)) \cong \pi_1(S^3 \setminus \nu(J)),$$

as desired.

To complete the proof, let $n \in \mathbb{N}$ be given, and choose J to be any knot with $\mathrm{rank}(\pi_1(S^3 \setminus \nu(J))) \geq n + 2$ (e.g. take J to be a connected sum of $n + 1$ trefoils [Wei98]). The exterior $S^4 \setminus \nu(Y)$ can be built relative to $\partial(S^4 \setminus \nu(Y)) \cong (S^1 \times S^2) \# (S^1 \times S^2)$ with some number of 4–dimensional 1–, 2–, 3–, and 4–handles. Since the 1–handles correspond to generators of the fundamental group, at least n are required; the boundary $\partial(S^4 \setminus \nu(Y))$ contributes only two to the rank of the fundamental group. Similarly, since we can obtain another presentation of $\pi_1(S^4 \setminus \nu(Y))$ with generators corresponding to 3–handles, the number of 3–handles in this decomposition is at least $n + 2$. $\square$

We note that the construction of $\mathcal{K}$ given in the above proof is closely related to an interesting construction of 2–knots given by Cochran [Coc83].

Next, we observe that many important examples of Seifert solids are, in fact, spinal:

(1) Every ribbon 2–knot bounds a Seifert solid Y that is homeomorphic to $(\#^m(S^1 \times S^2))^\circ$ for some m [Yan69]. The manifold Y is obtained by taking a Seifert surface F for some ribbon knot in an equatorial S^3, thickening it, and attaching trivial 2–handles above and below the equator. By attaching tubes to F (at the cost of increasing m), we can arrange for F to be free. Then Y is spinal.

(2) If $\mathcal{K}$ is fibered with fiber Y, then $S^4 \setminus \nu(Y) \cong Y \times I$ is an spinal, since Y is a punctured 3–manifold.

(3) Connected Seifert solids arising from broken surface diagrams via the construction given by Carter and Saito [CS97] are spinal. Recall that a connected, canonical Seifert surface is free because it deformation retracts to a graph so that on each edge, there is one local maximum and no local minima with respect to the radial height function on S^3. (Here, the vertices of the graph correspond to the disks produced in Seifert's procedure while the edges correspond to the half-twisted bands.) This ensures that the exterior of a canonical surface can be built with 0– and 1–handles. Similarly, a Seifert solid constructed à la [CS97] deformation retracts to a 2–complex with one local maximum and no other critical points in the interior of each 1– and 2–cell. Thus, the exterior of such a Seifert solid can be built with 0–, 1–, and 2–handles.

Finally, we can formulate a question analogous to the 3–dimensional results in [KK96] in the setting of surface-knots.

Question 4.3 *Define the* genus *of an orientable surface-knot S in S^4 to be the minimal first Betti number of any Seifert solid bounded by S, and define the* spinal genus *and* canonical genus *similarly, using spinal Seifert solids and canonical Seifert solids, respectively. Do there exist surface-knots for which these three measures of complexity differ?*

We remark that using techniques as in the proof of Theorem 4.2, one can show that for some of the known classical knots K whose genus and free genus are sufficiently different (see [Mor87], for example), the spun knots $S(K)$ admit low-complexity non-spinal Seifert solids, whereas the obvious spinal and canonical Seifert solids have greater complexity. However, it is likely to be considerably more difficult to obstruct the existence of low-complexity spinal or canonical Seifert solids, even for these examples.

5 On standardness of bridge trisections

The goal of this section is to prove Theorem 5.2, which states that a $(b; c_1, c_2, c_3)$–bridge trisection that satisfies $c_i \geq b - 1$ for some $i \in \mathbb{Z}_3$ can be completely decomposed into standard pieces. This proves Conjecture 4.3 of [MZ17], and the theorem can be viewed as the bridge trisection analog of the main result in [MSZ16], which states that every $(g; k_1, k_2, k_3)$–trisection with $k_i \geq g - 1$ for some i is standard in that it decomposes into genus one summands.

We encourage the reader to recall the notions of *perturbation* and *connected summation* for bridge trisections. The former was first introduced in Section 6 of [MZ17], where it was referred to as stabilization, and the latter can be reviewed in Subsection 2.2 of [MZ17]. See also [MTZ20, Section 3] for a succinct description of these concepts.

We call a surface-link an *unlink* if it is the split union of unknotted surface-knots, though we allow the topology of each component to vary. For example, one might have a 2–component

unlink that is the split union of an unknotted 2–sphere and an unknotted projective plane. (See Subsection 2.2 of [MTZ20] and Subsection 2.3 above for a brief discussion of unknotted surface-knots.)

Before proving Theorem 5.2 in generality, we recall the case in which $c_i = b$ for some $i \in \mathbb{Z}_3$. This was addressed as Proposition 4.1 of [MZ17]. A bridge trisection is called *completely decomposable* if it is a disjoint union of perturbations of one-bridge and two-bridge trisections.

Proposition 5.1 *[MZ17, Proposition 4.1] Let $\mathfrak{T}$ be a $(b; c_1, c_2, c_3)$–bridge trisection with $c_i = b$ for some $i \in \mathbb{Z}_3$. Then, $\mathfrak{T}$ is completely decomposable, and the underlying surface-link is the unlink of $\min_i\{c_i\}$ 2–spheres.*

Note that if $c_i = b$ for some $i \in \mathbb{Z}_3$, then $c_{i-1} = c_{i+1}$. Similarly, in what follows we will see that if $c_i = b - 1$ for some $i \in \mathbb{Z}_3$, then $|c_{i-1} - c_{i+1}| \le 1$. We now present and prove the main result of this section.

Theorem 5.2 *Let $\mathfrak{T}$ be a $(b; c_1, c_2, c_3)$–bridge trisection with $c_i = b - 1$ for some $i \in \mathbb{Z}_3$. Then, $\mathfrak{T}$ is completely decomposable, and the underlying surface-link is either the unlink of $\min\{c_i\}$ 2–spheres or the unlink of $\min\{c_i\}$ 2–spheres and one projective plane, depending on whether $|c_{i-1} - c_{i+1}| = 1$ or $c_{i-1} = c_{i+1}$.*

The key ingredient in the proof of the theorem is a pair of results of Scharlemann and Bleiler-Scharlemann about planar surfaces in 3–manifolds [Sch85, BS88]. We refer the reader to Section 1 of each of these papers, as we will adopt the notation of [Sch85, Theorem 1.1] and [BS88, Theorem 1.3] in the proof below.

Proof of Theorem 5.2 We induct on the bridge number b of the bridge trisection. When $b = 1$ or $b = 2$, there is an easy classification of b–bridge trisections [MZ17, Subsection 4.3], which we take as the base case. Assume the theorem holds when the bridge number is less than b, and let $\mathfrak{T}$ be a $(b; c_1, c_2, c_3)$–bridge trisection. Assume without loss of generality that $c_3 = b - 1$.

Suppose that $\mathcal{T}_1$, $\mathcal{T}_2$, and $\mathcal{T}_3$ are the three tangles comprising the spine of the bridge trisection. Every b–bridge splitting of a c–component unlink with $b > c$ is a perturbation of the standard c–bridge splitting of the c–component unlink, which is itself unique up to isotopy [MZ17, Proposition 2.3]. It follows that there exist collections Δ_1 and Δ_3 of bridge disks for $\mathcal{T}_1$ and $\mathcal{T}_3$, respectively, so that the shadows $\Delta_1^* = \Delta_1 \cap \Sigma$ and $\Delta_3^* = \Delta_3 \cap \Sigma$ have the property that $\Delta_1^* \cup \Delta_3^*$ is an embedded collection of $b - 2$ bigons and a single quadrilateral. Let α_0^* denote one of the arcs of Δ_1^* in the quadrilateral.

Let $L = \mathcal{T}_2 \cup \overline{\mathcal{T}}_3$, and let $\mathfrak{b}$ be the band for L that is framed by Σ and whose core is α_0^*. Then the data $(\Sigma, L, \mathfrak{b})$ encodes a banded b–bridge splitting, since the resolution $L_{\mathfrak{b}}$ is the

unlink $L' = \mathcal{T}_2 \cup \overline{\mathcal{T}}_1$. (Here, we think of $\flat$ as being slightly perturbed to lie in the 3–ball containing $\mathcal{T}_3$.) We refer the reader to Section 3 of [MZ17], especially Lemma 3.3, for more details about banded bridge splittings and how they arise from bridge trisections.

Assume without loss of generality that $c_2 = |L|$ is greater than or equal to $c_1 = |L'|$. We break the remainder of the proof into two cases: Either $c_2 > c_1$ or $c_2 = c_1$. Note that since there is only one band present, we must have $c_2 - c_1 \le 1$. The proofs of the two cases are very similar, except that we apply [Sch85, Theorem 1.1] in the first case and [BS88, Theorem 1.3] in the second.

Case 1. If $c_2 = c_1 + 1$, then $\flat$ connects distinct components K_1 and K_2 of L. Let K' denote the component of L' obtained as the resolution $(K_1 \cup K_2)_\flat$. We now translate this set-up into the notation of [Sch85, Section 1]. Let $N = \overline{\nu(K_1 \cup \flat \cup K_2)}$, a genus two handlebody, and let $M = S^3 \setminus \nu(L \setminus (K_1 \sqcup K_2))$. Let E_1 denote the spanning disk bounded by K_1. Let $P' = \partial\nu(E_1)$, a 2–sphere disjoint from $K_1 \sqcup K_2$ in M. Let Q' denote a spanning disk bounded by K' in M. Let $P = \overline{P' \setminus N}$, and let $Q = \overline{Q' \setminus N}$.

It is clear from this set-up that $P \cap \partial N$ is a collection of m parallel separating curves A_m for some odd m, since P' was disjoint from K_1 and K_2, but intersects $\flat$ transversely. (See [Sch85, Fig. 1].) Similarly, we have $Q \cap \partial N$ agrees with the curves B_n, since $\partial Q' = K'$ and Q' may crash through $\flat$ in arcs parallel to its core. Thus, M, N, P, and Q satisfy the hypotheses of [Sch85, Theorem 1.1]. The relevant conclusion is that A_1 and B_0 bound embedded disks E and F in $\overline{M \setminus N}$ that intersect in a single arc. (Compare with the proof of [Sch85, Main Theorem].)

Translating this conclusion back into the setting of interest, we find that the disk E is properly embedded in $S^3 \setminus \nu(\flat)$ and that F is a spanning disk for K'. This implies that the pair $(B^3, T) = (S^3, L) \setminus (\nu(\flat), \nu(L \cap \flat))$ is the split union of a trivial tangle and an unlink: The strands of the trivial tangle are parallel into push-offs of E via the components of $F \setminus \nu(E)$, at which point they are parallel into $\partial\nu(\flat)$ via the push-offs of E.

The bridge sphere Σ induces a bridge splitting (B^3, T). By Theorem 2.2 of [Zup13], Σ is either minimal for (B^3, T) or perturbed[1]. If the splitting were minimal, we would have $b = c_2$, so $\mathfrak{T}$ would be completely decomposable by Proposition 5.1. If the splitting is perturbed, then $\mathfrak{T}$ is perturbed, since each bridge arc of $\mathcal{T}_3$ that is disjoint from $\nu(\flat)$ is a strand of a 1–bridge splitting of a component of $L_3 = \mathcal{T}_3 \cup \overline{\mathcal{T}}_1$. After de-perturbing $\mathfrak{T}$, we find that $\mathfrak{T}$ is completely decomposable, by the inductive hypothesis.

Case 2. If $c_2 = c_1$, then $\flat$ connects a component K of L to itself. Let $K' = K_\flat$. We now translate this set-up into the notation of [BS88, Section 1], abbreviating the discourse where it is overly repetitive of the previous case. Let $M = S^3 \setminus \nu(L \setminus K)$, and let $N = \nu(K \cup \flat)$.

---

[1]Although Theorem 2.2 of [Zup13], as stated, applies to a closed 3–manifold M and a link K in M, a verbatim proof establishes the more general case where the 3–manifold M is replaced by a punctured 3–manifold and the link K is a tangle.

Let P' be a spanning disk bounded by K in M, and let Q' be a spanning disk bounded by K' in M. Let $P = \overline{P' \setminus N}$, and let $Q = \overline{Q' \setminus N}$.

It is clear from the set-up that the hypotheses of [BS88, Theorem 1.3] are satisfied, so we can conclude that some A_0 and B_0 bound embedded disks E_P and E_Q, respectively, in $\overline{M \setminus N}$. Moreover, there is a properly-embedded disk D in $\overline{M \setminus N}$, disjoint from E_P and E_Q, that runs once over one of the handles of N and is disjoint from the other handle. We can extend E_P to a spanning disk F for K. (Compare with the proof of [BS88, Theorem 1.8].)

The strands of $K \setminus \nu(\mathfrak{b})$ are parallel into push-offs of D via the components of $E_P \setminus \nu(D)$, at which point they are parallel into $\partial \nu(\mathfrak{b})$ via the push-offs of D. It follows that the tangle $(B^3, T) = (S^3, L) \setminus (\nu(\mathfrak{b}), \nu(\mathfrak{b} \cap K))$ is the split union of a trivial tangle and an unlink, and Σ gives rise to a bridge splitting of (B^3, T). As before, this splitting is either minimal or perturbed. The case that the splitting is perturbed has the same consequence as in Case 1 above.

If the splitting is minimal, then it is a split union of a 2–bridge splitting of the trivial tangle and a $(b - 2)$–bridge splitting of an unlink. It follows that the bridge trisection is a split union: $\mathfrak{T} = \mathfrak{T}' \sqcup \mathfrak{T}''$, where $\mathfrak{T}'$ is a $(2, 1)$–bridge trisection (of a projective plane, necessarily), and $\mathfrak{T}''$ is a $(b - 2; c_1 - 1, c_2 - 1, b - 2)$–bridge trisection (of an unlink of 2–spheres, necessarily). The latter is completely decomposable by Proposition 5.1. $\qquad\square$

We can also use Theorem 5.2 to understand surface-links with particular banded link presentations, where a *banded link presentation* (L, v) consists of an unlink $L \subset S^3$ and a collection of bands v such that the resolution L_v of L along v is also an unlink. Every banded link presentation gives rise to a surface $\mathcal{S}$ in S^4, and conversely, every surface-link $\mathcal{S}$ in S^4 can be presented by a banded link [KSS82].

In [MZ17, Section 3], the authors introduced the notion of *banded bridge splitting* of (L, v), a bridge splitting of L such that the bands v are isotopic into the bridge sphere with the surface framing and are dual to a collection of bridge disks on one side. They showed that $(S^4, \mathcal{S})$ admits a $(b; \mathbf{c})$–bridge trisection if and only if a banded link presentation (L, v) of $\mathcal{S}$ admits a banded b-bridge splitting such that $|L| = c_1$, $|v| = b - c_2$, $|L_v| = c_3$. As a corollary to Theorem 5.2, we obtain the following, which states, in essence, that a surface is unknotted if the bands are attached in a relatively simple way to the maxima or minima disks.

Corollary 5.3 *Suppose a surface-link $\mathcal{S}$ in S^4 is presented by a banded link (L, v) with a banded b–bridge splitting such that $b = |L| + 1$ or $b = |L_v| + 1$. Then $\mathcal{S}$ is an unlink of 2–spheres or an unlink of 2–spheres and an unknotted projective plane.*

The corollary exploits a feature of trisection theory called *handle triality*: If (L, v) admits a banded bridge splitting as in the corollary, then it admits a $(b, \mathbf{c})$–bridge trisection such that

$c_1 = b - 1$ or $c_3 = b - 1$. By the three-fold symmetry of the trisection setup, we can extract a different banded link presentation with a single band, as in the proof of Theorem 5.2, and now we rely on known results about surface-links built with a single band to classify $\mathcal{S}$. The result can be interpreted as an analog for knotted surfaces of Theorem 1.2 from [MSZ16].

References

[BS88]   Steven Bleiler and Martin Scharlemann, *A projective plane in* $\mathbf{R}^4$ *with three critical points is standard. Strongly invertible knots have property P*, Topology **27** (1988), no. 4, 519–540.

[Coc83]   Tim Cochran, *Ribbon knots in* S^4, J. London Math. Soc. (2) **28** (1983), no. 3, 563–576.

[CS97]   J. Scott Carter and Masahico Saito, *A Seifert algorithm for knotted surfaces*, Topology **36** (1997), no. 1, 179–201.

[DM23]   Irving Dai and Maggie Miller, *The 0-concordance monoid admits an infinite linearly independent set*, Proc. Amer. Math. Soc. **151** (2023), no. 8, 3601–3609.

[GK16]   David Gay and Robion Kirby, *Trisecting 4-manifolds*, Geom. Topol. **20** (2016), no. 6, 3097–3132.

[GL78]   C. McA. Gordon and R. A. Litherland, *On the signature of a link*, Invent. Math. **47** (1978), no. 1, 53–69.

[Glu62]   Herman Gluck, *The embedding of two-spheres in the four-sphere*, Trans. Amer. Math. Soc. **104** (1962), 308–333.

[Gor76]   C. McA. Gordon, *Knots in the* 4*-sphere*, Comment. Math. Helv. **51** (1976), no. 4, 585–596.

[JMMZ22]   Jason Joseph, Jeffrey Meier, Maggie Miller, and Alexander Zupan, *Bridge trisections and classical knotted surface theory*, Pacific J. Math. **319** (2022), no. 2, 343–369.

[KK96]   Masako Kobayashi and Tsuyoshi Kobayashi, *On canonical genus and free genus of knot*, J. Knot Theory Ramifications **5** (1996), no. 1, 77–85.

[KSS82]   Akio Kawauchi, Tetsuo Shibuya, and Shin'ichi Suzuki, *Descriptions on surfaces in four-space. I. Normal forms*, Math. Sem. Notes Kobe Univ. **10** (1982), no. 1, 75–125.

[Liv82]   Charles Livingston, *Surfaces bounding the unlink*, Michigan Math. J. **29** (1982), no. 3, 289–298.

[Miy86]   Katura Miyazaki, *On the relationship among unknotting number, knotting genus and Alexander invariant for* 2*-knots*, Kobe J. Math. **3** (1986), no. 1, 77–85.

[Mor87]   Yoav Moriah, *On the free genus of knots*, Proc. Amer. Math. Soc. **99** (1987), no. 2, 373–379.

[MSZ16]   Jeffrey Meier, Trent Schirmer, and Alexander Zupan, *Classification of trisections and the generalized property R conjecture*, Proc. Amer. Math. Soc. **144** (2016), no. 11, 4983–4997.

[MTZ20]   Jeffrey Meier, Abigail Thompson, and Alexander Zupan, *Cubic graphs induced by bridge trisections*, to appear in Math. Res. Letters, available at arXiv:2007.07280, July 2020.

[MZ17]   Jeffrey Meier and Alexander Zupan, *Bridge trisections of knotted surfaces in* S^4, Trans. Amer. Math. Soc. **369** (2017), no. 10, 7343–7386.

[MZ18] _____ , *Bridge trisections of knotted surfaces in 4-manifolds*, Proceedings of the National Academy of Sciences **115** (2018), no. 43, 10880–10886.

[Sch85] Martin Scharlemann, *Smooth spheres in* $\mathbf{R}^4$ *with four critical points are standard*, Invent. Math. **79** (1985), no. 1, 125–141.

[Tsa92] Chichen M. Tsau, *A note on incompressible surfaces in solid tori and in lens spaces*, Knots 90 (Osaka, 1990), de Gruyter, Berlin, 1992, pp. 213–229.

[Wei98] Richard Weidmann, *On the rank of amalgamated products and product knot groups*, Math. Ann. **312** (1998), no. 4, 761–771.

[Yan69] Takaaki Yanagawa, *On ribbon* 2-*knots. The* 3-*manifold bounded by the* 2-*knots*, Osaka Math. J. **6** (1969), 447–464.

[Zee65] E. C. Zeeman, *Twisting spun knots*, Trans. Amer. Math. Soc. **115** (1965), 471–495.

[Zup13] Alexander Zupan, *Bridge and pants complexities of knots*, J. Lond. Math. Soc. (2) **87** (2013), no. 1, 43–68.

Department of Mathematics, North Carolina School of Science and Mathematics, Morganton, NC, USA

Department of Mathematics, Western Washington University, Bellingham, WA, USA

Department of Mathematics, University of Texas at Austin, Austin, TX, USA

Department of Mathematics, University of Nebraska-Lincoln, Lincoln, NE, USA

jason.joseph@ncssm.edu, jeffrey.meier@wwu.edu, maggie.miller.math@gmail.com, zupan@unl.edu